High Power WDM Sources for Laser Communication

Matthew Welch[a], Aubin Donnot[a], James Edmunds[a], Marios Kechagias[a], Elliot Prowse[a], Karen Hall[a], Peter Kean[a], and Efstratios Kehayas[a]

[a]G&H, Broomhill Way, Torquay, United-Kingdom

ABSTRACT

The next generation high bandwidth optical links from earth to space will requirement the development of new high power WDM sources. In this paper G&H present the latest results of their ongoing development of these sources. Namely the development and testing of a 50W optical fibre amplifier that operates across much of C-band is presented as well as a high power wavelength division multiplexer, designed to combine multiple high power amplifiers outputs into a diffraction limited beam.

Keywords: Feeder links, Optical Ground Station, Free Space Optical Communication, FSOC, Optical Fibre Amplifier, Spectral Beam Combiner, WDM, VERTIGO

1. INTRODUCTION

Constellations of satellites that employ laser communications are rapidly being developed. These satellites distribute data across the constellation at very high bandwidths (Gbit/s) utilising relatively low optical powers (Watts), due to space providing a near perfect transmission medium for optical communication. High bandwidth laser communication into (and out of) these space borne constellation from earth, are necessary for the majority of use cases. These optical links however must contend with the effects of atmospheric scatter, mitigations based on adaptive optics[1] or multiple transmit apertures can be employed[2] - however ultimately higher optical powers must be employed than for space borne applications.

Optical powers at $1.55\mu m$ are limited by amplifier technology and therefore the highest data rate terrestrial to space links are being designed around wavelength division multiplexing of multiple optical amplifiers.[3] In this paper G&H report their progress in increasing the power of optical communications amplifiers in this wavelength range to 50W. In addition progress in developing high power wavelength division multiplexers for combining these sources is also reported.

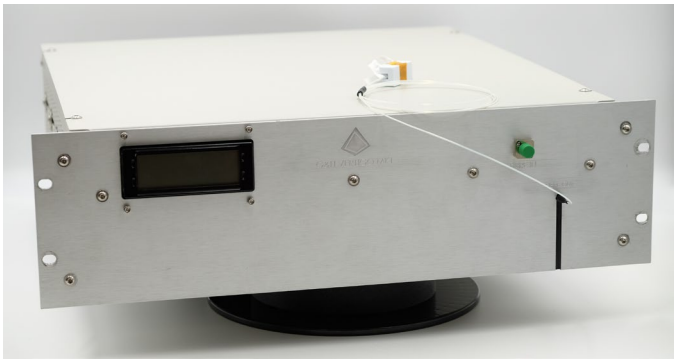

Figure 1: Photograph of 50W optical amplifier, designed around a 19" rack compatible form factor.

Further author information: (Send correspondence to M.W.)
M.W.: E-mail: MWelch@gandh.com

This work was supported by the H2020-SPACE-VERTIGO project from the European Union's Horizon 2020 research and innovation program under grant agreement No. 822030. This is an accepted version of the manuscript submitted to SPIE for publication. Posting of accepted versions is permitted under SPIE sharing policies: https://www.spiedigitallibrary.org/article-sharing-policies.

Citation: Matthew Welch, Aubin Donnot, James Edmunds, Marios Kechagias, Elliott Prowse, Karen Hall, Peter Kean, Stratos Kehayas, "High power WDM sources for laser communication," Proc. SPIE 11993, Free-Space Laser Communications XXXIV, 119930B (4 March 2022); https://doi.org/10.1117/12.2608506

2. 50W C-BAND AMPLIFIER

2.1 Design

Optical amplification of a 1mW data signal to 50W requires the provision of 47dB of gain. To provide stable, power efficient amplification across a range of wavelengths whilst achieving this high level of gain, a design with multiple amplifications stages is necessitated. One possible design for a 50W, 4-stage amplifier is shown in figure 2. The design incorporates an initial 976nm core pumped erbium doped fibre amplifier stage to stably provide up to 23dB of gain, amplifying a 1mW tunable source to 200mW. The signal is then amplified by 10dB to 2W, and then by 7dB to 10W, in double clad amplifier stages utilizing (10/125μm) Erbium (Er)/Ytterbium (Yb) doped fibre, cladding pumped at 940nm. A subsequent Large Mode Area (LMA) (25/300 μm), double clad Er/Yb fibre amplifier, cladding pumped at 940nm provides 7dB of gain to achieve the required 50W signal level. LMA fibre being employed to suppress paracistic lasing at 1μm at the high pumping level required[4] and suppress the nonlinear effect of Stimulated Brillouin Scattering (SBS).[5]

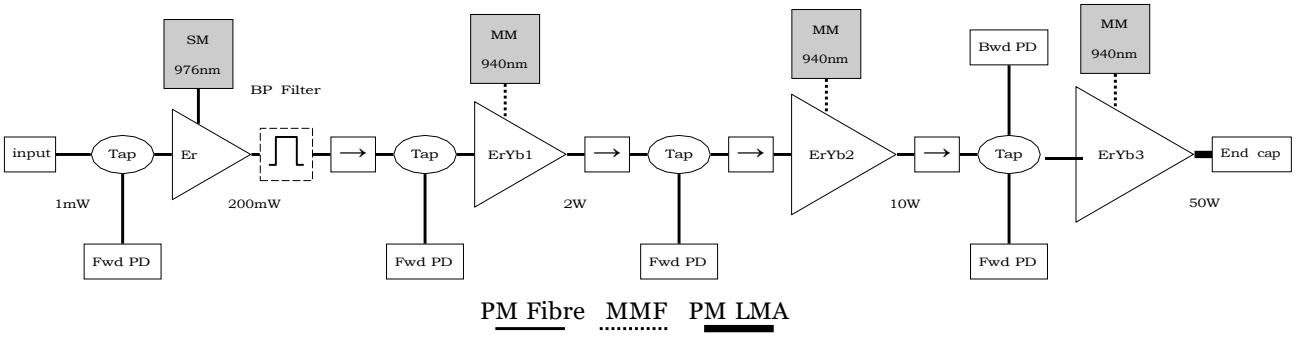

Figure 2: Schematic of 50W C-Band Amplifier. To ensure stable operation the non LMA amplifier stages are protected by isolators and with photodiodes being provided to monitor performance. The LMA amplifier stage is protected from backreflections by an endcap, with a photodiode also being provided to monitor the level of backwards propagating light. The bandpass filter shown, was not included in the 19" rack units shown in figure 1 but is included here to aid discussed in the following section.

The design employs polarisation maintaining fibre throughout the signal path, and outputs a linearly polarised, diffraction limited beam. A beam expanding end-cap is employed at the output to reduce reflections into the final amplifier stage and reduce the risk of failure at the interface. Two amplifiers of this design were manufactured and packaged into 19" housings to allow shipment and testing by partners in the H2020 VERTIGO[3] project that is developing Tbit/s feeder links, figure 1.The first three amplification stages have a combined electrical power consumption of 77.3W for a 10W optical signal entering the final LMA amplifier stage. This LMA amplifier stage then has electrical to optical conversion efficiency of ≈ 22% leading to the electrical to optical consumption curves shown in figure 3. Noise figures of 7.11dB & 7.29dB were measured in two separate amplifier builds, for a 1mW 1564nm signal amplified to 50W.

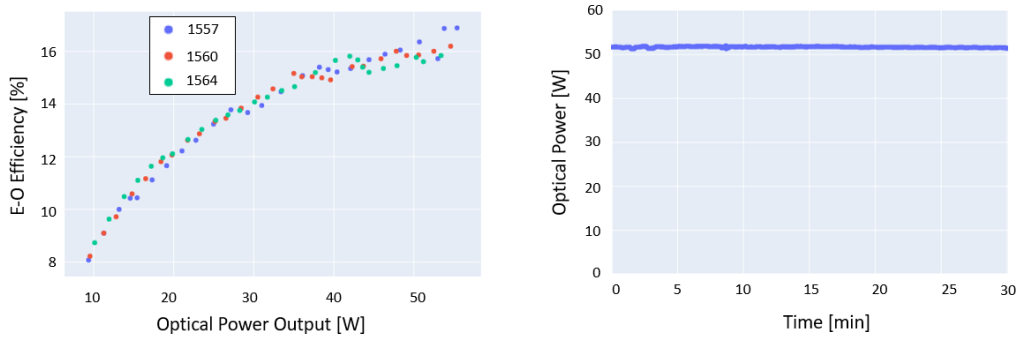

Figure 3: 50W amplifier electrical to optical conversion efficiency, and power log over 30min ($\sigma = 0.11W$)

2.2 Amplified Spontaneous Emission (ASE) Suppression

It is notable that the 47dB of gain provided by the 50W amplifier is similar to that of the low noise high gain receiver amplifiers that G&H have provided for spaceborne lasercomm applications; these receive amplifiers amplifying (≈ -55dBm signals to 0dBm levels).[6] At this high gain level, the 50W amplifier experiences the same issues of spectral gain dependence as the aforementioned receive amplifiers. Specifically the 4 stage amplifier provides its peak gain towards the long wavelength edge of the C-band, at 1560-1565nm. The simulated gain peak for a "free-running"/no input configuration was at 1562nm - see figure 5. If the signal wavelength differs from this gain peak wavelength, ASE at the gain peak will receive greater gain than that of the signal. For signal wavelengths detuned from the gain peak by $\rangle\ 10nm$ the output power can contain ASE power (> 5%), with the amplification of ASE reducing the signal amplification. Figure 4a shows both experimental and numerical simulations of the ratio of output ASE power to signal power for the 50W amplifier as function of input wavelength. Amplification across the C-band is truncated particularly at short wavelengths. Figure 4b shows experimental and simulation results for the inclusion of 1nm FWHM tunable bandpass filter after the first amplifier stage (as shown in figure 2). Setting this filter to the signal wavelength suppresses paracistic ASE amplification and one can observe that amplification to 50W with low ASE content can be achieved across much of C-band. Simulations showing the viability of this gain continuing to shorter wavelengths in the L-band. Figure 4c shows experimentally measured spectra for the filtered amplifier for a signal wavelengths from 1542nm to 1569nm.

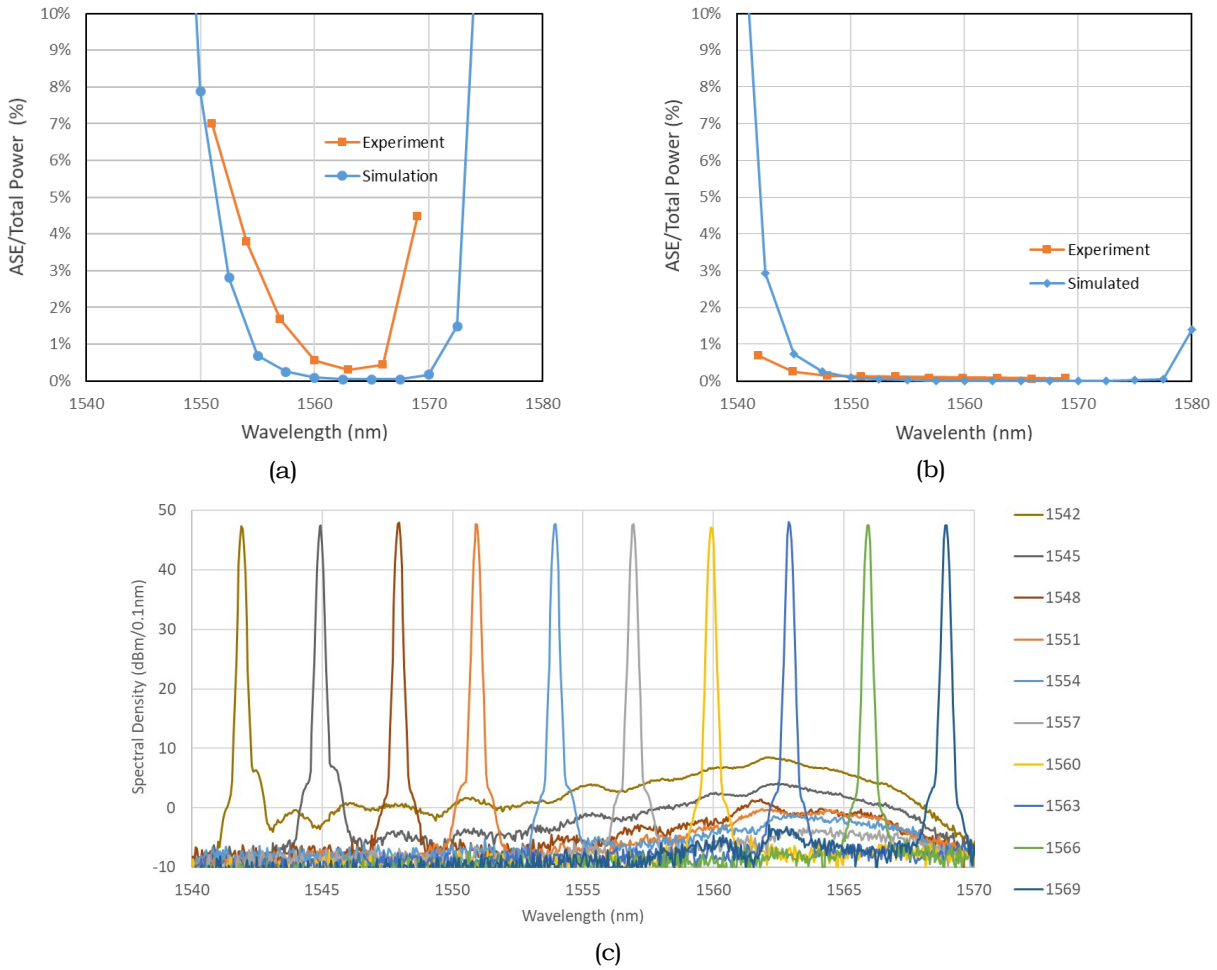

Figure 4: Simulated and experimentally measured ASE content of 50W amplifier as function of input wavelength. Data produced for a 1mW input, for a configurations without & with ASE filtering in 4a & 4b respectively. 4c Output spectral for the filtered configuration at 50W output power for 1mW input.

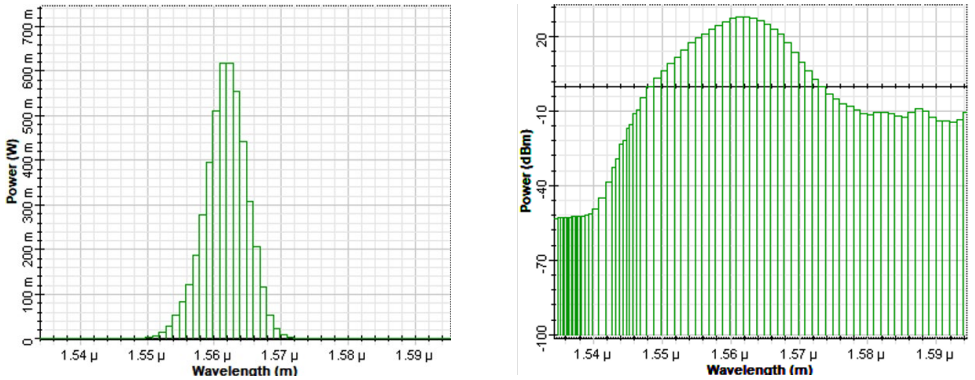

(a) Linear Scale (b) Logarithmic Scale

Figure 5: Simulated output spectra for 50W amplifier when seeded with no input signal, power is shown employing an 0.1nm resolution.

2.3 Thermal Management

Though the 50W of optical power produced is modest compared to kW class optical amplifiers/lasers that are widespread at $1\mu m$, thermal loads are typically much higher in Er/Yb than Yb amplifiers for a given output power. The two key reasons for this are that, firstly the quantum defect for $1.55\mu m$ Er/Yb amplifiers is approximately $4\times$ that of $1.55\mu m$ Yb amplifiers (for 940nm pumping). Secondly higher dopant levels are typically employed in commercially available Er/Yb fibres than Yb fibre, pump absorption being typically $>3\times$ greater.

Under a balanced bi-directional pumping configuration of the final amplifier stage we estimate the peak heat load in the active fibre for $50\,W$ output is $19\,W.m^{-1}$. Experimentally we measured a maximum temperature increase of this fibre of 12.8K, leading to an assumed heat sinking performance of the active fibre of $0.67K.m.W^{-1}$. It is likely that this value exceeds our expected value of $\approx 0.4K.m.W^{-1}$ obtained through finite element analysis due to splice imperfections, figure 6a. The value however does leave ample overhead to scale the output power amplifier well beyond 50W, whilst maintaining fibre temperatures well below manufacture cited maximum temperatures of $120^{\circ}C$.

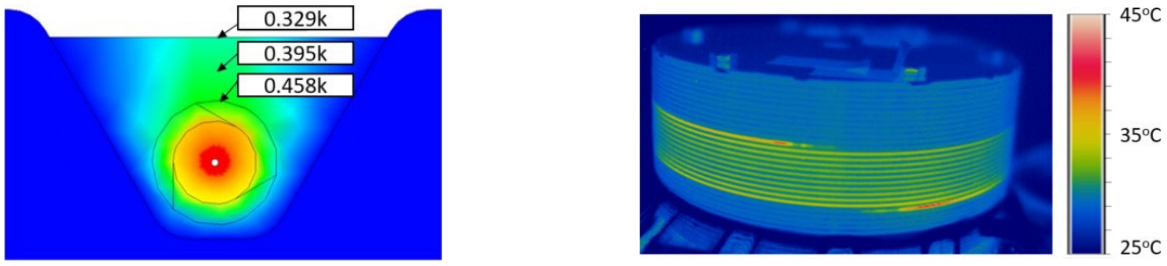

(a) (b)

Figure 6: 6a Simulated cross section of the active fibre temperature rise for the heat sinking arrangement employed, simulated for a heatload of $1\,W.m^{-1}$ in the fibre core. 6b Thermal image of the fibre operating at 50W, the fibre is balanced bi-bidirectionally pumped with $2\times70\,W$ of pump, leading to an estimated peak thermal load of $19\,W.m^{-1}$. The maximum fibre temperature was $12.8^{\circ}C$ above the heatsink temperature of $\approx 30^{\circ}C$.

2.4 50W Amplifier Conclusion

The viability of amplifying linearly polarised diffraction limited 1mW signals by 47dB to 50W across much of the C-band has been shown. Numerical simulation show feasibility of the extending amplification into the L-band, and a thermal analysis shows the feasibility of additional power scaling to higher power levels.

3. HIGH POWER SPECTRAL BEAM COMBINER

3.1 Introduction

Terrestrial telecomms Wavelength Division Multiplexing (WDM) components for mW power levels are widespread, with high channel count multiplexers being produced in small form factor packages. These components however are not capable of withstanding the power levels required for high power WDM systems for satellite communication. To this end, in this section G&H present their work towards producing a spectral combiner/multiplexer to fulfil this requirement.

In generality there are two approaches that can be employed for spectral combination. Either an angular dispersive element is employed - where light is deflected by an angle that depends in its frequency, or a reflective approach is employed - whereby light is transmitted/reflected depending on its frequency. Neither approach is idealised, each having its merits in terms of parameters such as physical size, scalability to high channel count, viable channel bandwidth and channel spacing. The design outlined below and shown in figure 7 & 8 is based upon commercially available fused silica transmission gratings as angular dispersive elements.

Three linearly polarised, fibre coupled high power collimators, outputting beam diameters of 2.1mm are steered to propagate coaxially onto the first grating, with the beams being spaced on a 3.9 mm pitch. They are incident on the 1000 lines/mm grating at an angle of 50°. For the 300GHz frequency spacing between channels this leads to 1.05m "walk on distance" for the beams to overlap on the the second grating, where they again propagate coaxially. This beam is then steered and attenuated before being incident on a beam profiler.

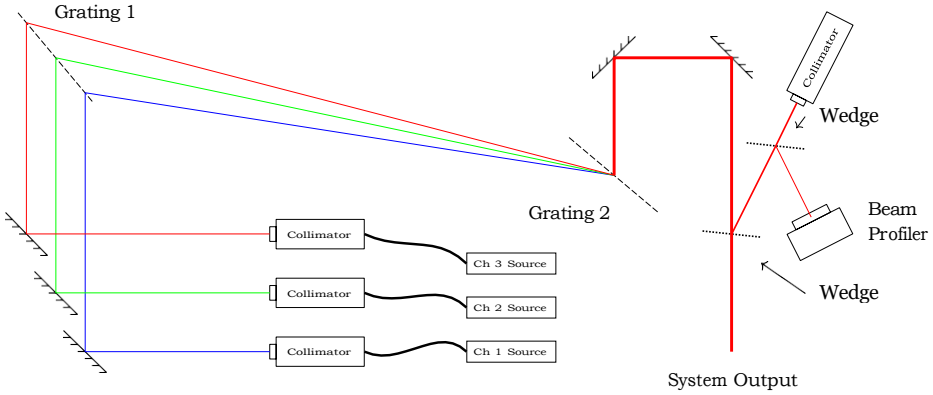

Figure 7: Spectral Beam Combiner Schematics

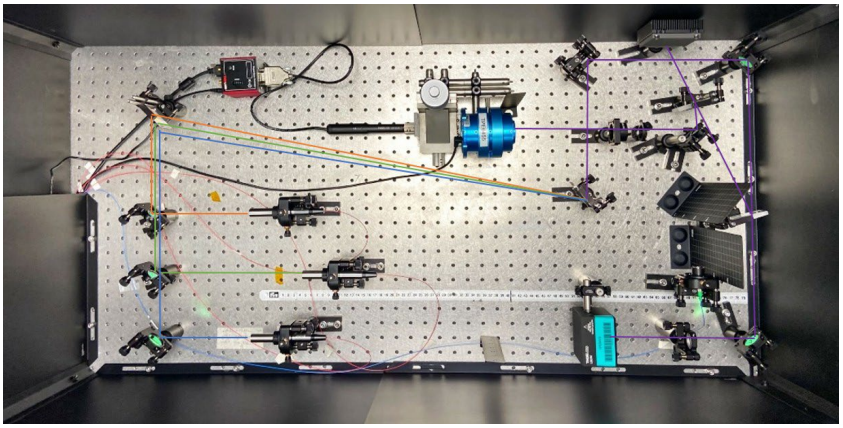

Figure 8: Image of Spectral Beam Combiner (SBC), superimposed on the image are the beam paths from the 3 collimators (shown in orange/green/blue) and combined beam (purple). Power from this combined beam is picked off using fused silica wedges and then directed to a spinning slit beam profiler for characterisation.

3.2 Key Design Considerations

Like any system there are a large number of competing design considerations, this section provides a brief overview of their interplay. A key limitation of architectures based on angular dispersive elements, is that frequency components of a given channel are diffracted at different angles. To this end as the bandwidth of input channels increase, beam quality decreases. The architecture outlined employs a pair of gratings in a rhomb configuration as mitigation to this effect. In this rhomb configuration, an increase in channel bandwidth leads to an enlargement of the spot size on the second grating, but does effect the coaxial prorogation from this grating. Madasamy *et al.*,[7] perform an analysis of the beam quality degradation for such an architecture that employs a pair of gratings. They show that for channel line widths of $\Delta\lambda$ the output M^2 can be approximated as:

$$M^2 = 1 + \frac{x\Delta\lambda}{2\omega_0\,(\lambda_n - \lambda_{n+1})} \tag{1}$$

Where ω_0 is the input beam diameter (2.1mm), $(\lambda_n - \lambda)$ is the wavelength spacing between channels (≈2.4nm), and x is the spacing of coaxial beams incident on the first grating (3.9mm). For an example channel bandwidth of 0.1nm, near diffraction limited performance is still viable, with a limit of $M^2 > 1.04$ being predicted.

One can observe that a tighter pitch between the coaxial beams on first grating would lower M^2 degradation with channel bandwidth. This would however lead to increased clipping of power beam on steering mirrors. A 3.9mm pitch with 2.1mm beam diameter was selected such that perfect alignment would reduce this loss to 0.1%; though as discussed later in practice this value was much larger. The small beam diameter selected (2.1mm) was chosen to minimise the walk on length (1.05m). It is sufficiently large to control the incident power density on the components below damage thresholds, and allow for beam collimation to be maintained through the optical path. The 1.05m walk on length could in a finalised design be folded several times to produce a more compact design.

3.3 Results

"Low Power" measurements were initially done to characterise the performance of the system, this was done using 3 tuneable optical sources each with 13dBm power and a linewidth of < 10kHz. In this configuration transmission losses of between 17% and 11.5% were measured for the 3 input channels. The majority of these losses are due to the clipping of the input beams on the edges of steering mirrors. M^2 measurements have been taken using a spinning slit beam profiler following the ISO 11146:2005 standard.[8] Figure 9a shows an example of M^2 measurement for the combination the aforementioned three 13dBm powers each with < 10kHz linewidth. In these results the x-axis is the the dispersive axis, for which a slightly larger M^2 is measured, $M^2_x = 1.08 \pm 0.02$; $M^2_y = 1.04 \pm 0.01$. Though these results are slightly above that of a perfectly diffraction limited beam, they still represent excellent beam quality for this application.

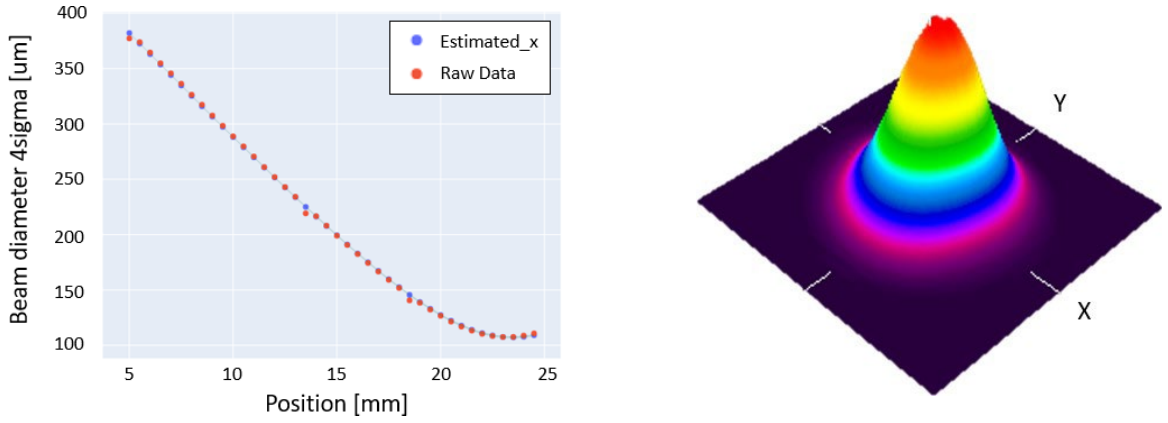

(a) M^2 measurement of beam in dispersed (x-axis) (b) Example intensity plot

Figure 9: Beam Profile Measurements of the combination of low power channels.

To assess the sensitivity of the spectral combiner to line width broadening affecting the output beam quality; one of the three 13dBm channels was detuned from its central frequency, (the other two channels non being detuned). The effect on the combined M^2 of the three channels is shown in figure 10. It can be observed that the M^2 only increases for the dispersed (x) axis, with it remaining constant for the non dispersed (y) axis. To check for beam degradation linked to the use of higher optical powers a 10W source was employed. Characterisation at higher powers and with multiple sources is envisaged in the future. Within the margin of error of our measurement no change in M^2 or focal position in the M^2 measured could be detected with increasing the launched power (figure 11), nor could any increase in thermal signatures in be detected with via IR/thermal imaging.

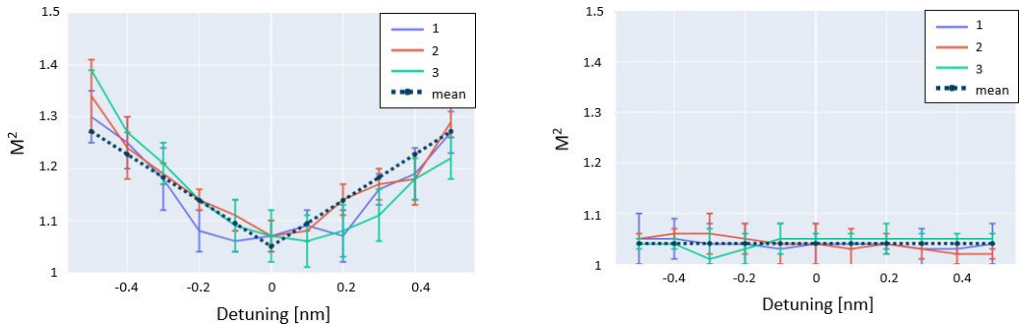

(a) Dispersed (x) axis (b) Non dispersed (y) axis

Figure 10: Measurements of M^2 for 3 channels, where 1 channel is detuned from its central frequency.

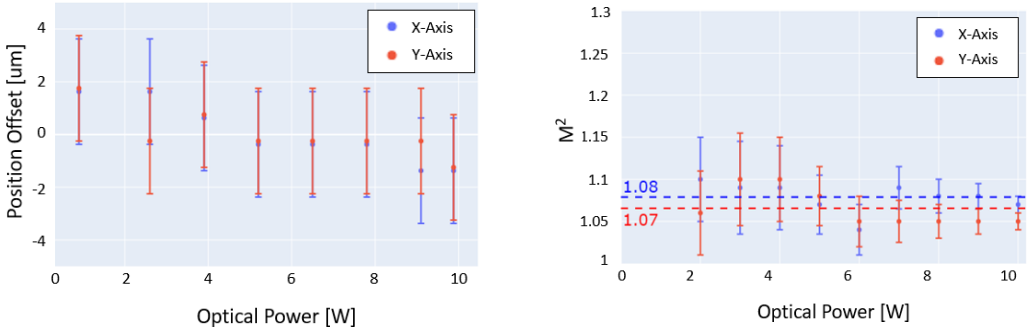

(a) Evolution of Beam Centroid Position (b) Evolution of M^2

Figure 11: Evolution of Beam Parameters with Power for a single 10W channel.

3.4 Spectral Beam Combiner Conclusion

A 3 channel, rhomb grating pair spectral combiner has been assembled and tested. Near diffraction limited beam quality was achieved with narrow line width inputs, the increase in M^2 with channel detuning being characterised. No degradation in performance with optical power was observed with the 10W source employed.

4. CONCLUSION

We presented in this paper G&H's latest work toward producing High Power Wavelength Division Multiplexing (WDM) sources for laser communications that will be employed as part of demonstrators in the VERTIGO project. We report results of a C-band 50W Optical Fiber Amplifier (OFA), showing the the viability of 50W power generation across the C-band and into the L-band. We also have reported work into producing a High Power Spectral Beam Combiner (SBC), capable of handling three 10W channels whilst maintaining near diffraction limited performance.

ACKNOWLEDGMENTS

The authors also acknowledge support from the VERTIGO project, which has received funding from the European Union's Horizon 2020 research and innovation program under grant agreement No. 822030. The authors also acknowledge support from the Engineering and Physical Sciences Research Council grant number EP/S022821/1, and doctoral support from Dr. G. Flockhard & Prof. C. Michie at the University of Strathclyde.

REFERENCES

[1] Kaushal, H. and Kaddoum, G., "Optical Communication in Space: Challenges and Mitigation Techniques," *IEEE COMMUNICATIONS SURVEYS AND TUTORIALS* **19**(1), 57–96 (2017).

[2] Silvestri, F., Pettazzi, F., Eschen, M., Boschma, J. J., Lutgerink, J. B., Kramer, G. F. I. J., Korevaar, W. C., den Breeje, R., Duque, C. M., and Doelman, N. J., "Beam multiplexing for satellite communication optical feeder links," in [*Free-Space Laser Communications XXXII*], Hemmati, H. and Boroson, D. M., eds., **11272**, 245 – 253, International Society for Optics and Photonics, SPIE (2020).

[3] Kernec, A. L., Canuet, L., Maho, A., Sotom, M., Matter, D., Francou, L., Edmunds, J., Welch, M., Kehayas, E., Perlot, N., Krzyzek, M., Paraskevopoulos, A., Leuthold, J., Horst, Y., Bourderionnet, J., Brignon, A., Lallier, E., Billault, V., Leviandier, L., Conan, J.-M., V´edrenne, N., Lim, C. B., Montmerle-Bonnefois, A., Petit, C., Stampoulidis, L., Fehrenz, M., and Lehnigk-Emden, T., "The H2020 VERTIGO project towards tbit/s optical feeder links," in [*International Conference on Space Optics — ICSO 2020*], Cugny, B., Sodnik, Z., and Karafolas, N., eds., **11852**, 508 – 519, International Society for Optics and Photonics, SPIE (2021).

[4] Matniyaz, T., Kong, F., Kalichevsky-Dong, M. T., and Dong, L., "302 W single-mode power from an Er/Yb fiber MOPA," *OPTICS LETTERS* **45**, 2910–2913 (MAY 15 2020).

[5] Zeringue, C., Dajani, I., Naderi, S., Moore, G. T., and Robin, C., "A theoretical study of transient stimulated brillouin scattering in optical fibers seeded with phase-modulated light," *Opt. Express* **20**, 21196–21213 (Sep 2012).

[6] Edmunds, J., Henwood-Moroney, L., Hammond, N., Prowse, E., Hall, K., Szemendera, L., Davoudzadeh, N., Holland, P., Simpson, K., Palmer, C., Stampoulidis, L., Kean, P., Welch, M., and Kehayas, E., "Miniaturized modules for space-based optical communication," in [*Free-Space Laser Communications XXXIII*], Hemmati, H. and Boroson, D. M., eds., **11678**, 109 – 118, International Society for Optics and Photonics, SPIE (2021).

[7] Madasamy, P., Jander, D., Brooks, C., Loftus, T., Thomas, A., Jones, P., and Honea, E., "Dual-grating spectral beam combination of high-power fiber lasers," *IEEE Journal of Selected Topics in Quantum Electronics* **15** (2009).

[8] "ISO 11146-1:2005 - Lasers and laser-related equipment — Test methods for laser beam widths, divergence angles and beam propagation ratios — Part 1: Stigmatic and simple astigmatic beams," standard, International Organization for Standardization, Geneva, CH (Jan. 2005).